Slip-Based Tire-Road Friction Estimation ⋆

Fredrik Gustafsson [1]

Department of Electrical Engineering, Linköping University, S-581 83, Linköping, Sweden.

Tire-road friction is estimated using the wheel-slip computed from standard sensor signals. A parametric model is estimated using an adaptive filter supported by a fault detector. Results from extensive field trials are presented.

An approach to estimate the tire–road friction during normal drive using only the wheel slip, that is, the relative difference in wheel velocities, is presented. The driver can be informed about the maximal friction force and be alarmed for sudden changes. Friction related parameters are estimated using only signals from standard sensors in a modern car. An adaptive estimator is presented for a model linear in parameters, which is designed to work for periods of poor excitation, errors in variables, simultaneous slow and fast parameter drifts and abrupt changes. The physical relation between these parameters and the maximal friction force is determined from extensive field trials using a Volvo 850 GLT as a test car.

Key words: automotive control, adaptive filters, fault detection, classification, Kalman filters

1 Introduction

Tire—Road Friction Estimation (TRFE) has become an intense research area as the interest of information technology in vehicles increases. For instance, the need of

⋆ Submitted to Automatica 960120, revised 960807 and re-revised 961127

[1] Email: fredrik@isy.liu.se. Fax: +46-13282622. This work was done as a part of the project *Driver Assistance and Local Traffic Management* in the Swedish RTI program '91-'94. Main sponsors are The Swedish Board for Industrial and Technical Development, AB Volvo, Saab-Scania AB and The Swedish National Road Administration.

TRFE is established as the problem area "Common European Demonstrator 2.1", Friction Monitoring and Vehicle Dynamics, in the European Prometheus project and it is also identified by the Advanced Vehicle Control Systems Committee of the Intelligent Vehicle Highway Society of America ([1]). TRFE is of importance in itself as a driver information unit, but friction information is also needed in other functions like safety margin determination, autonomous intelligent cruise control, collision avoidance systems and for exchange of road-side information.

To our knowledge, four different approaches to TRFE have been tried:

- Use the so called wheel slip, that is, the difference in wheel velocities of driven and non-driven wheels.
- Use optical sensors installed at the very front of the car. The reflections from the surface are used to estimate the road surface and possible lubricants. This approach has the advantage of being able to estimate the friction slightly before the tires reach for instance an icy spot. A difficulty here is to keep the sensors clean.
- Acoustic sensors can be used to listen to the tire noise, which gives some information about the surface.
- Supply the tires' tread with sensors for measuring stress and strain. This solution is technically very complicated and expensive.

The last three approaches are investigated in [2]. The use of optical and acoustic sensors is particularly promising for detecting wet surfaces and risk for aqua-planing. The use of acoustic sensors in combination with a neural net is examined in [3]. There are also methods for estimating the friction during excitation, for instance using an active ABS system as described in [4].

In this work, we follow the first approach. It should be remarked that this approach has been tried at least twice only in Sweden with a negative result, probably due to insufficient measurement accuracy and filtering techniques. Recently, the relation between wheel slip and friction was reported in [5] for several tires and some different surfaces. Perhaps the most important feature is that only existing sensors are needed if the car is supplied with ABS brakes. It works for two-wheel driven vehicles and during normal driving, but not when braking. The goal is to compute certain parameters from available standard sensors in the car, which depend directly or indirectly on the friction, and to find rules how to evaluate the maximal friction forces that can be used for braking or cornering. There are two problems of theoretical interest in this approach:

- Design an adaptive parameter estimator suitable for this application. It must give accurate estimates and at the same time be able to track fast variations.
- Determine the physical relation between these parameters and the maximal friction forces.

We will here focus on the first problem and briefly summarize the results of the tests.

The basic assumption on a relation between slip and friction is in fact in contradiction to classical tire friction theory, but it has been supported in [5] and it is strongly confirmed in this work and empirical evidence will be presented. However, the difference in slip on different surfaces is quite small, which might be the reason why this relation has not been discovered until recently.

The filter used in [5] is based on a time average of one parameter. To compute this, another parameter needs to be estimated, which is done during free-rolling. The proposed filter is based on modern model based signal processing where both these parameters are estimated simultaneously and adaptively and no free-rolling is needed. Furthermore, a change detection algorithm is used for detecting and estimating abrupt changes quickly. Another major contribution here is a systematic test plan including many winter tests on ice and snow, which are two surfaces not tested at all in [5].

An introduction and summary of the project can be found in Section 2. The outline follows the signal flow depicted in Figure 1. The block labeled "Measuring" represents the metrology. The measured quantities are used to compute physical quantities in a straightforward manner as detailed in Appendix A. These quantities are in the next block used to filter out parameters related to the friction. The critical design of the filter is presented in Section 3. In the last block, the filtered parameters are used to classify what the friction is. To design a classifier a large number of tests is required, and the results of these are summarized in Section 4. Finally, conclusions are found in Section 5. Readers only interested in parameter estimation for this application can skip Section 4, while readers not familiar with estimation theory may skip Section 3, since Section 2 provides the context in both cases. A short version of this work was presented in [6].

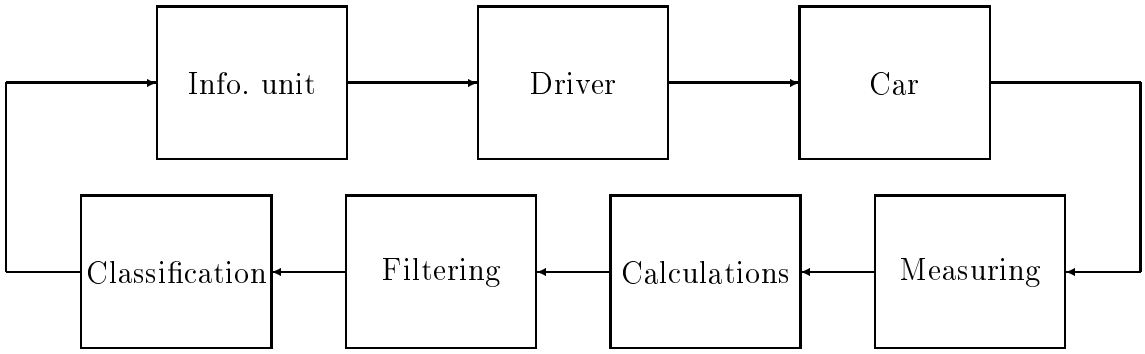

Fig. 1. Signal flow

2 A brief outline

This section is a short guide to the content of this work where the most important quantities for friction estimation are defined.

The basic idea in the chosen approach is to study the friction dependency in the so called *slip*. The slip is defined as the relative difference of a driven wheel's circumferential velocity, $\omega_w r_w$, and its absolute velocity, v_w:

$$s = \frac{\omega_w r_w - v_w}{v_w}, \tag{1}$$

where r_w is the wheel radius. This is the definition suggested in [7]. Another common definition is $s = \frac{\omega_w r_w - v_w}{\omega_w r_w}$, see *e.g.* [8]. For small slip values, as considered here, these definitions give almost the same value.

The absolute velocity of a driven wheel is computed from the velocities of the two non-driven wheels and geometrical relations in a straightforward manner.

We also define the friction coefficient (μ) as the ratio of traction force (F_f) and normal force (N) on one driven wheel,

$$\mu = \frac{F_f}{N}. \tag{2}$$

A plot of the friction coefficient versus the slip, $\mu = \mu(s)$, shows a very significant characteristics which depends on the combination of tire and road. Examples on slip curves are sketched in Figure 2. We are of course interested in the maximal friction

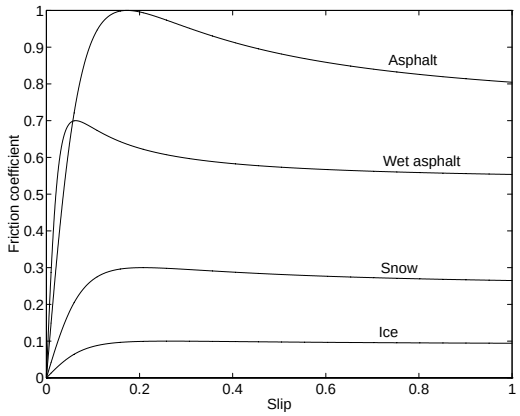

Fig. 2. Schematic plots of μ–s curves for different surfaces. The inital slope is exaggerated.

coefficient μ_{max}, but during normal driving only small values $\mu < 0.2$ are observed. The question is if these observations can be used to predict μ_{max}.

Figure 3 shows examples of test drives on asphalt and ice, respectively. Visual in-

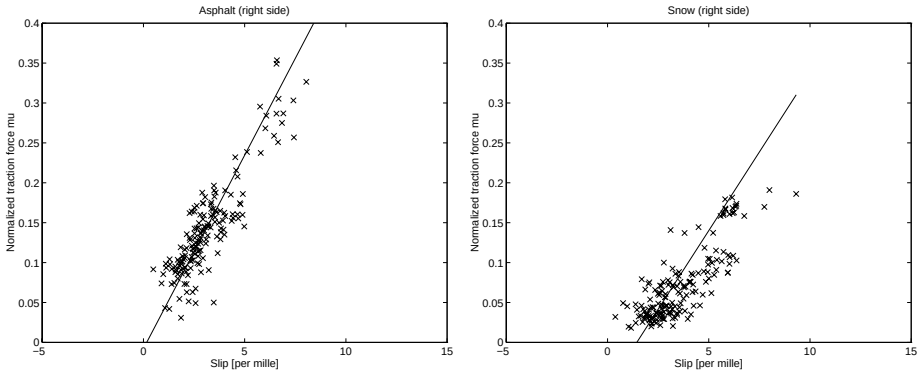

Fig. 3. Samples of μ and s, computed from ABS signals on the right side of the car, on dry asphalt (left) and hard snow (right), respectively. Crosses denote measurements and the solid line is a straight-line approximation.

spection reveals a slight difference in slope, so we define

$$k = \left.\frac{d\mu}{ds}\right|_{\mu=0} \tag{3}$$

This slope k is commonly referred to as the *longitudinal stiffness* since it can be justified theoretically from the tire characteristics alone. A stiff tire gives a large k. Since this theory does not explain the friction dependency, we prefer to call it simply the *slip slope*. The hypothesis is that

– the slip slope contains sufficiently much information to provide an accurate value of the friction (μ_{max}).

The slip slope is estimated from the straight-line assumption $\mu = ks$ for small slip values. We stress that standard models of the μ–s relation, like the physical one outlined in [8] and the model $\mu = ks/(as^2 + bs + 1)$ in [9], have constant initial slope. A more general model $D\sin(C\arctan(B((1-E)s + E/B\arctan(BX))))$ suggested in [10] was used to generate the artificial curves in Figure 2.

When trying to compute the slip from the linear approximation $s = \mu/k$ in (3), one will notice a significant offset (not illustrated in Figure 2),

$$\delta = \left. s \right|_{\mu=0}. \tag{4}$$

That is, the slip is not zero when the traction force is zero. This is mainly due to a

small difference in effective wheel radii, and must be compensated for when the slip slope is estimated. Much of the details in the algorithm concern questions how to compensate for this offset, cornering *etc* when computing the slip.

The precision of the estimates of k and δ hinges on the quality of the data. Apart from abnormal measurements, the data quality is effectively assessed by the variation in $\mu(t)$ to be defined later. If the variation is small, the estimates will be stochastically uncertain and the slip slope might be overestimated as well. That is, to get reliable estimates the driver should change the position of the gas pedal regularly.

If only the slip slope was used to estimate the friction, we would face problems on gravel roads. It has turned out that the slip slope can take on almost any value on gravel. Before going on, we make the following assumptions about gravel roads:

- Of course the driver knows when he is driving on gravel. We still need to detect gravel, partly in order not to confuse him by random friction information and partly because other functions might need the information.
- We do not intend to distinguish different frictions levels on gravel.

The very course surface texture on gravel roads opens a possibility to classify gravel separately. The surface's coarseness gives a random contribution to the measurement of the angular velocity. Consider the relation between the angular velocity of one free-rolling wheel and its horizontal velocity

$$\omega_w = v_w/r_w + e. \tag{5}$$

That is, v/r_w is the angular velocity one would get on a perfectly even surface. Now, we can define

$$\gamma = 4 \ \mathrm{Var}(e) \tag{6}$$

and use it for detecting gravel. The factor 4 will be explained later.

To conclude this discussion, we have three quantities which *could* depend on the friction: k, δ, γ. Suppose now that we make a number of test drives on surfaces with known properties. We can then illustrate each test as a point in the space (k, δ, γ). To each point we hang on a surface label. Then, omitting the offset δ, we get for instance a plot as shown in Figure 4. This and similar tests are presented in Section 4. It is clear from the figure that we can construct a classifier which works for this car and these tires and at this time. For instance, the following classifier can be used:

Gravel ($\mu \approx 0.5$) if $\gamma > 0.027$.

Asphalt ($\mu > 0.8$) if $\gamma < 0.027$ and $k > 30$.
Snow or ice ($\mu < 0.3$) if $\gamma < 0.027$ and $k < 30$.

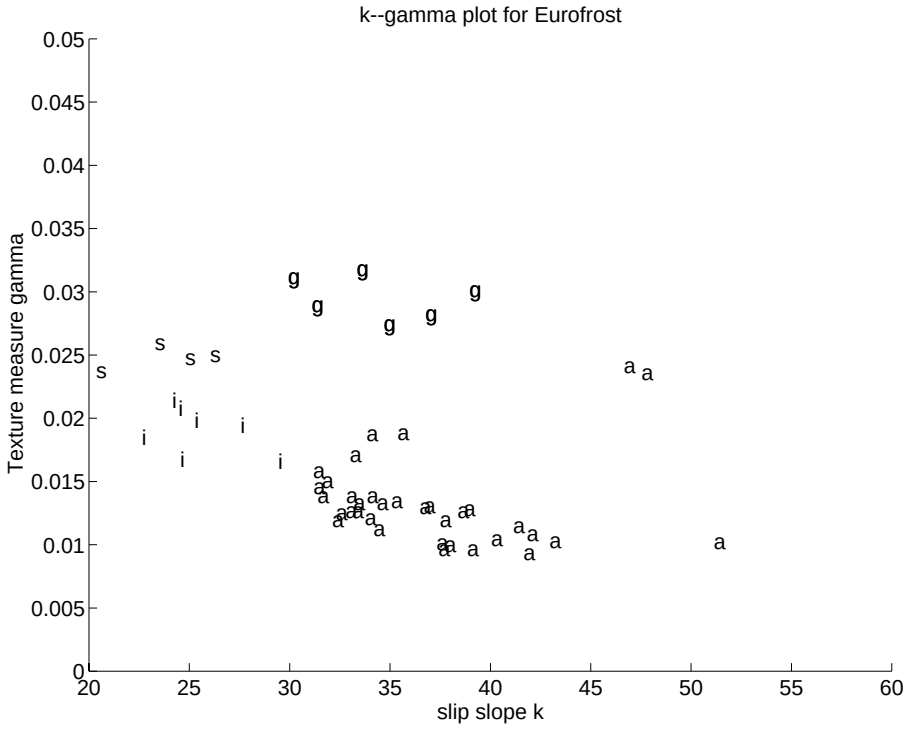

Fig. 4. Slip slope and texture measure as a function of surface for the winter tire "Eurofrost". The markers stand for asphalt (a), snow (s), ice (i) and gravel (g).

As indicated above, it is not at all sure that this classifier works half a year later, or with different tires or even on another car. This implies that the classifier has to be adaptive, which is a major problem. However, detection of slow and abrupt changes in friction is still possible.

3 Filtering

In this section, we will assume that we have measurements of the slip s and the normalized traction force $\mu = F_f/N$. An index m will be used to distinguish the measured quantities from the true ones. Both s and μ are computed, without filtering, from measured quantities as described in Appendix A.

The slip slope k we want to compute is defined in (3) which for small μ reads (using (4))

$$\mu = k(s - \delta) \tag{7}$$

where also δ is unknown. The approach in [5] is to estimate δ separately during free-rolling, when $\delta = s$, and then compute k from (7) directly, or some moving average value to increase the accuracy. One drawback with this two-step method is that δ may vary with the surface, and this might cause problems. The averaging introduces an undesired estimation delay, and the tradeoff between estimation accuracy and short time delay is tricky. Here, we will make use of sophisticated filtering where k and δ are estimated simultaneously. The design goals are

- to get accurate values on k while keeping the possibility to track slow variations and at the same time
- detect abrupt changes in k rapidly.

This will be solved by a Kalman filter supplemented by a failure detection algorithm.

3.1 Time-invariant estimation

To begin with, we will formulate the problem as a time-invariant one. This allows us to gain useful insight into the problems that may occur in the general case, and will also simplify the derivation of the time-varying estimator. We can also think intuitively of time-varying estimation as a time-invariant one over a short data window.

3.1.1 Choosing a linear regression model

Equation (7) expressed as

$$\mu = ks - k\delta \tag{8}$$

is a linear model for s and μ, where k and $k\delta$ are two unknown parameters. However, there are two good reasons for rewriting it as

$$s = \mu\frac{1}{k} + \delta. \tag{9}$$

That is, we consider s to be a function of μ rather than the other way around. The reasons are

- The measurement noise variance is much larger for s than for μ. We will mostly neglect the latter uncertainty. In that case the measurement noise will be additive to (9) while it is multiplied by k in (8).

– Both parameters k, δ are time-varying, where k is supposed to vary much faster than δ. This implies that (8) has two rapidly changing parameters k and $k\delta$ while (9) will have one rapidly and one slowly varying parameter, which is a much easier filtering problem.

Introducing measurement noise on s, we get the following *linear regression model*:

$$\begin{aligned} s_m(t) &= \mu(t)\frac{1}{k} + \delta + e(t) \\ &= (\mu(t)\ 1)\begin{pmatrix} \frac{1}{k} \\ \delta \end{pmatrix} + e(t) \\ &= H(t)x + e(t). \end{aligned} \tag{10}$$

Here $x = (1/k, \delta)^T$ is a vector of unknown parameters, $H(t)$ is a regression vector $(\mu(t), 1)$ and $e(t)$ is a term to catch measurement errors and model mismatch where it will be assumed that $e(t)$ is white noise with variance σ^2. There are two linear regression models (10), one for each driven wheel.

3.1.2 The least squares estimate

Classical least squares theory gives that the best parameter estimate that can be formed from N measurements of $s_m(t)$ and $H(t)$ is given by

$$\hat{x}_N = \left(\sum_{t=1}^{N} H^T(t)H(t) \right)^{-1} \sum_{t=1}^{N} H^T(t)s_m(t) \tag{11}$$

The measure of fit

$$\widehat{\sigma^2} = \frac{1}{N}\sum_{t=1}^{N}(s_m(t) - H(t)\hat{x}_N)^2 \tag{12}$$

is the natural estimate of measurement error variance.

In the next two subsections we analyse two problems that may not only occur here, but also in the general time-varying case.

3.1.3 Biased estimates caused by errors in $\mu(t)$

A well-known problem in the least squares theory occurs in the case of errors in the regression vector. This is usually referred to as *errors in variables* or the *total least*

squares problem, see [11]. In our case, we have measurement and computation errors in the normalized traction force $\mu(t)$. Assume that

$$\mu_m(t) = \mu(t) + v_\mu(t), \quad \mathrm{Var}(v_\mu(t)) = \lambda_\mu \tag{13}$$

is used in $H(t)$ in (11). Here $\mathrm{Var}(v_\mu(t))$ means the variance of the error in the measurement $\mu_m(t)$. It can easily be shown that it leads to a positive bias in the slip slope

$$\hat{k} \approx k \frac{\overline{\mathrm{Var}}(\mu) + \lambda_\mu}{\overline{\mathrm{Var}}(\mu)} > k \tag{14}$$

Here $\overline{\mathrm{Var}}(\mu)$ is the variation of the normalized traction force defined as

$$\overline{\mathrm{Var}}(\mu) = \frac{1}{N}\sum_{t=1}^{N} \mu_t^2 - \left(\frac{1}{N}\sum_{t=1}^{N} \mu_t\right)^2. \tag{15}$$

This variation is identical to how one estimates the variance of a stochastic variable. Normally, the bias is small because $\overline{\mathrm{Var}}(\mu) >> \lambda_\mu$. That is, the variation in traction force is much larger than its measurement error.

3.1.4 Uncertain estimates caused by lack of excitation

A conceptually different phenomenon is caused by the same reason as the parameter bias. The quality of the estimates is namely also related to the variation of traction force.

The covariance matrix of the parameter estimate is

$$P_N = \mathrm{Cov}(\hat{x}_N) = \sigma^2 \left(\sum_{t=1}^{N} H^T(t)H(t)\right)^{-1}. \tag{16}$$

If the matrix to be inverted is close to singularity, its inverse will be large and the estimates very uncertain. We can check how close this matrix is to singularity by computing its determinant

$$\det\left(\sum_{t=1}^{N} H^T(t)H(t)\right) = \det\begin{pmatrix} \sum_{t=1}^{N}\mu^2(t) & \sum_{t=1}^{N}\mu(t) \\ \sum_{t=1}^{N}\mu(t) & \sum_{t=1}^{N} 1 \end{pmatrix}$$

$$= N \sum_{t=1}^{N} \mu^2(t) - \left(\sum_{t=1}^{N} \mu(t) \right)^2$$
$$= N^2 \overline{\mathrm{Var}}(\mu(t)). \tag{17}$$

That is, if the variation in traction force is small during the time constant of the filter (N here), the parameter uncertainty will be large.

3.1.5 Influence of driving style

To investigate the influence of driving style, a number of tests were performed where three different possibilities were compared:

- Poor excitation and a constant velocity of 70 km/h.
- Poor excitation and a constant velocity of 90 km/h.
- High excitation. The speed was changed back and forth between 70 km/h and 90 km/h.

The same asphalt road was used in all tests and they were all performed on the same day. Table 1 summarizes the result.

According to the discussions in subsections 3.1.3 and 3.1.4 low excitation could give a bias and uncertain estimates. This is confirmed in Table 1 where high excitation gives an extremely small variation between different drives (small standard deviation) and a slip slope that is significantly smaller than for the non-exciting drives.

Tire	70 km/h	90 km/h	High excitation	Number of tests
MXT	52.5 (1.6)	53.8 (2.3)	48.7 (0.7)	4
Eurofrost	39.9 (2.1)	35.0 (3.3)	33.2 (0.8)	10

Table 1
Mean and standard deviation of estimated slip slope for different driving styles

3.1.6 What to do during poor excitation

An intuitive explanation to the two aforementioned problems is as follows: If the variation of $\mu(t)$ is very small during the time constant of the filter (N), we are effectively collecting data clustered around one and only one point in a (k, s) plot. A straightline approximation of these data points can then take on almost any slope and offset. Ideally, the driver should switch traction force between one large and one small value. Then it would be easy to get an accurate estimate of the slip slope. This is also the philosophy in many of the test drives in Section 4.

A remedy to the problems caused by lack of excitation in traction force is suggested as follows: In the car we have access to almost infinitely many data. We also know that the parameter δ is almost constant. These two facts mean that each time we start a time-invariant estimation as in (11) over a short time window there is very certain prior information about δ available. If we know that the traction force is not excited sufficiently, we could turn off the tracking ability of δ and concentrate on estimating time-variation in k only, until the excitation gets better. There would be no bias nor uncertainty caused by lack of excitation then.

The only remaining task is to decide when the variation of $\mu(t)$ is large enough to assure good performance of (11). The noise variance λ_μ can be considered as a constant depending only on the engine. A rough estimate of λ_μ can be obtained from data. This is done by using two test drives on the same road the same day, one with very poor and one with good excitation. The well excited one gave $\hat{k} \approx k \approx 84$, while the poorly excited one gave $\mathrm{Std}(\mu) = 0.009$ and $\hat{k} = 148$. A time-invariant estimator is used and there are many samples (N large) so the estimates are fairly accurate according to (17). Equation (14) now gives $\lambda_\mu = 0.009^2(148/84 - 1) = 0.008^2$. To have, say, less than 10 % bias, we must require that

$$\overline{\mathrm{Var}}(\mu) > \frac{0.008^2}{0.1} = 6.4 \cdot 10^{-4} \approx 0.025^2. \tag{18}$$

This limit has been confirmed to be effective in practice. It also gives an upper bound on the stochastic uncertainty in the estimated slip slope, as follows from (17).

3.2 Time-varying estimation

We will now allow time variability in the parameters, $k(t)$ and $\delta(t)$. Basically, there are three methods to estimate time-varying parameters, namely Least Mean Squares (LMS), Recursive Least Squares (RLS) with forgetting factor and the Kalman filter, see [12] for instance. All these methods contain some design variable to tune the time constant of the filter. This time constant can then be interpreted as the data size N used in the previous section, and the bias (14) and variance (17) measures can be evaluated, at least approximately.

LMS is much too slow for this application. RLS has just one degree of freedom to adjust the adaptivity. We propose to use the Kalman filter, because it is easily tuned to track parameters with different speeds. To estimate the model quality parameters σ, $\mathrm{Var}(\mu)$ and the texture measure γ simple lowpass filters of their momentary values are used.

3.2.1 The Kalman filter

Equation (10) is extended to a state space model where the parameter values vary like a random walk. At the same time, we introduce one independent model for each driven wheel:

$$\begin{aligned} x(t+1) &= x(t) + v(t) \\ y(t) &= H(t)x(t) + e(t) \end{aligned} \tag{19}$$

where

$$\begin{aligned} Q(t) &= \mathrm{E}v(t)v^T(t) \\ R(t) &= \mathrm{E}e(t)e^T(t) \\ y(t) &= \begin{pmatrix} s_{m,l}(t) \\ s_{m,r}(t) \end{pmatrix} \\ H(t) &= \begin{pmatrix} \mu_l & 0 & 1 & 0 \\ 0 & \mu_r & 0 & 1 \end{pmatrix} \\ x(t) &= \left(\frac{1}{k_l(t)},\ \frac{1}{k_r(t)},\ \delta_l(t),\ \delta_r(t) \right)^T . \end{aligned}$$

The indeces l and r refer to left and right side of the car, respectively. Here $v(t)$ and $e(t)$ are considered as independent white noise processes. With this assumption, the Kalman filter (see [13]) gives the optimal (in the minimum variance sense) state estimates $\hat{x}(t)$:

$$\begin{aligned} S(t) &= P(t-1) + Q(t-1) \\ K(t) &= S(t)H^T(t)\left(H(t)S(t)H^T(t) + R(t)\right)^{-1} \\ \hat{x}(t) &= \hat{x}(t-1) + K(t)\left(y(t) - H(t)\hat{x}(t-1)\right) \\ P(t) &= S(t) - K(t)H(t)S(t). \end{aligned} \tag{20}$$

Here $P(t)$ is interpreted as the covariance matrix of the parameter estimates.

3.2.2 Choosing the design parameters

The Kalman filter equations contain four free matrices, the initialization $x(0), P(0)$ and the noise covariance matrices $Q(t), R(t)$.

Initialization is not a problem in this application since the filter is running since it was started the first time. Each time the car's engine is turned off the filter states are stored and used when the car is started again.

The well-known and quite tricky problem is how to determine feasible values on the covariance matrices $Q(t)$ and $R(t)$. Concerning irrelevant scalings of the covariance matrices, it is well-knonw that it is only the ratio $\|Q\|/\|R\|$ that matters, so one of them can be normalized. Here we take $R(t) = I$. It is assumed that the parameters vary independently, so we can write

$$Q(t) = \text{ diag}\left(q_k(t),\ q_\delta(t),\ q_k(t),\ q_\delta(t)\right). \tag{21}$$

Another idea, not investigated here, is to assume dependence between the slip slope of the left and right side, so $Q_{13} = Q_{31} > 0$. The magnitudes of $q_k(t)$ and $q_\delta(t)$ decide the time constants for estimating k and δ, respectively. The variation in wheel radii reflected in δ can be assumed to be rather slow compared to the variation in $k(t)$, which must be allowed to vary rather rapidly due to the problem formulation. On the other hand, we have no prior information about when large variations can be expected, so we can choose $Q(t) = Q$ time-invariant. Thus we choose $q_k >> q_\delta$. The actual magnitude of the elements of Q is chosen such that the time constant for estimating k is of the order a minute and about ten times larger for δ.

Relating this design choice to the discussion on parameter bias and estimation uncertainty, we can conclude that good excitation depends on how much the traction force has changed, roughly, the last ten minutes.

3.2.3 The CUSUM detector

The tracking ability is proportional to the size of the entries of Q. The Kalman filter is required to give quite accurate values on the slip slope and must by necessity have small values on the entries of Q, see [13]. On the other hand, we want the filter to react quickly to sudden decreases in k due to worse friction conditions. This is solved by running a failure detection algorithm in parallel with the Kalman filter. If it indicates that something has changed, then all entries of Q are increased to a large value, yielding a time constant less than a second for estimating the slip slope.

There are many conceivable change detection algorithms. The main candidates are the CUSUM test, see [14] or [15] for a thorough treatment, and the Generalized Likelihood Ratio (GLR) test, see [16] or [17] for some recent ideas.

– The CUSUM test is computationally very simple, intuitively easy to understand and can be motivated to be fairly robust to modeling errors and the different types of changes (abrupt or incipient) that can occur here.

– The GLR test requires parallel filters, delivers an estimate of the change and has the potential to locate the change time accurately. The last two properties are a bit questionable for incipient changes.

The CUSUM test is proposed here, mainly because of its simplicity. See [18] for a comparison of different change detection algorithms for this particular problem. In words, the CUSUM test looks at the prediction errors $\varepsilon_t = s_m(t) - H(t)\hat{x}(t)$ of the slip value. If the slip slope actually has decreased, we will get predictions that tend to underestimate the real slip. The CUSUM test gives an alarm when the recent prediction errors have been sufficiently positive for a while. Mathematically, the test is formulated as the following time recursion:

$$\begin{aligned} g_0 &= 0 \\ g_t &= g_{t-1} + \varepsilon_t - \nu \\ g_t &= \max(g_t, 0) \\ \text{if } g_t &> h \text{ then alarm and } g_t = 0 \end{aligned} \tag{22}$$

where ν and h are design parameters. This test is known to have a number of good properties, robustness being one of them. After an alarm, the state noise covariance matrix $Q(t)$ is increased a factor, allowing quick tracking in the Kalman filter. Since it will take at least one more sample until the Kalman filter converges and the driver can be informed about the new situation, such an alarm about a decrease in friction potential should immediately be delivered to the driver.

The CUSUM test (22) gives an alarm only if the slip slope decreases. A similar test is used also for an increasing slope, using two other design parameters ν and h. However, an alarm in this test is not important to the driver.

3.3 Example of filter response

In this section, an example is given to illustrate the interaction between the Kalman filter and the change detector, using data collected at the test track CERAM, Paris. A road with a sudden change from asphalt to gravel and then back to asphalt is considered. Figure 5 shows the estimated slip slope as a function of time in one of the tests, where the gravel path starts after 7 seconds and ends after 16 seconds.

Note that the Kalman filter first starts to adapt to a smaller slip slope but after 3 samples (0.6 s) something happens. This is where the CUSUM detector signals for an alarm and we have convergence after one more sample. A similar behavior is noted at the end of the gravel path. The Kalman filter first increases k slightly and after some samples it speeds up dramatically and it takes a couple of seconds

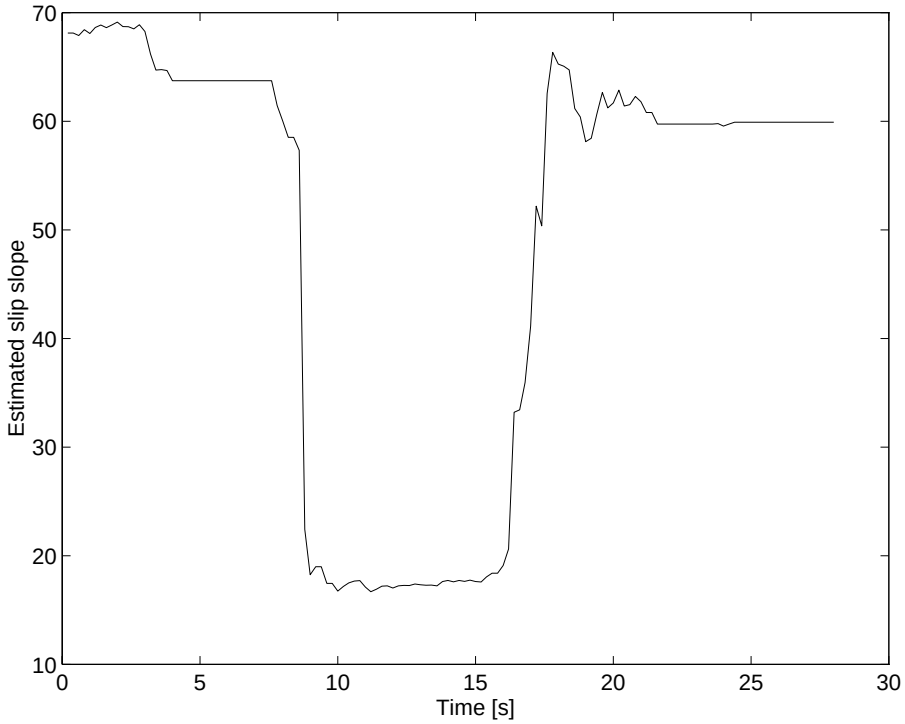

Fig. 5. Slip slope as a function of time. After 7 s an asphalt road changes to a short gravel path that ends at 16 s.

to converge to a stable value.

3.4 Outliers and model mismatch

Due to a number of reasons, some measurements of μ and s are useless. In these cases, the filter should be made inactive, which can be formulated mathematically (but not practically) as letting $Q(t) = 0$ and $R(t) = \infty$. Therefore, a number of more or less heuristic rules concerning the validity of the engine torque model, normal force and curve radius computation and friction model are used.

3.5 A measure of surface coarseness

Basically, it should be possible to classify gravel roads by its rough surface. Consider for instance the high frequency content of a non-driven wheel velocity. This is clearly a measure of the surface texture and it is large when the surface is uneven. On the other hand, it is also a function of the velocity of the car. Accelerations and especially a discontinuity in the velocity measurement at 8 km/h in the ABS sensors give a contribution as well, so soft driving on gravel might be classified as asphalt, while

wild driving on asphalt with many starts and stops could be mixed up with gravel. The approach outlined below has overcome these difficulties.

During one sample interval of 0.2 seconds, corresponding to approximately 4 meters for a velocity of 20 m/s, many small holes and ridges in the surface add up to a total error. According to the central limit theorem, this error will be Gaussian. This line of argumentation is supported by data as an example in [19] shows. A good model is that the true angular velocity on the left and right non-driven wheel, respectively, is a sum of a velocity dependent term and noise. Rewriting (5) we get

$$\omega_l(t) = v_l(t)/r_w + e_l(t)$$
$$\omega_r(t) = v_r(t)/r_w + e_r(t)$$

The variance of e_l and e_r contains information about the coarseness of the surface. That is, to detect gravel we would like to estimate the size, or variance, of e_l and e_r (which should be of the same magnitude on both sides normally). A natural idea is to study the difference $\omega_l - \omega_r$ which is independent of the velocity as long as the car is going straight ahead (when $v_l = v_r$).

However, in curves there will be a small bias caused by the difference in $v_l - v_r$. If this difference is constant in time, its influence can be removed by considering the time difference. That is, we propose to estimate the following quantity

$$\gamma = \mathrm{E}(\omega_l(t) - \omega_r(t) - \omega_l(t-1) + \omega_r(t-1))^2 \tag{23}$$

to detect gravel. The variance γ will be four times larger than the variance of e, which explains the factor 4 in (6). The point is that $\omega_l(t) - \omega_r(t) - \omega_l(t-1) + \omega_r(t-1)$ has zero mean when the turn rate is constant or when the car is going straight ahead, so $\mathrm{E}(\cdot)^2 = \mathrm{Var}(\cdot)$. An alternative to (23) is presented in [19], but it is not yet clear how to implement that algorithm recursively.

4 Test drives

The friction estimator was developed in parallel with test drives. It has been running more than 15000 km on the test car, a Volvo 850 GLT. About 1000 data files have been saved in test drives both on public roads under various conditions and on test tracks in Gothemburg (owned by Volvo), Arvidsjaur (TEVES), Wolfsburg (Volkswagen) and Paris (Renault/Matra). Among these, 300 have been put in a database for automated analysis. Here a fraction of these are presented.

4.1 Preliminaries

Tests on the following surfaces and tires will be presented.

- *Surface:* asphalt (a), wet asphalt (w), gravel (g), snow (s) and ice (i) determined by visual inspection.
- *Tire:* MXT, MXV2 (almost worn out), NCT2, and Eurofrost (winter tires).

The discussion will be in terms of slip slope k and the texture parameter γ. It is important to note the following assumptions in the estimation.

- The filter starts from the same initial condition in each test drive. This simplifies a direct comparison. The initial covariance matrix $P(0)$ is chosen large to get a short transient.
- The filter assumes time invariance, that is, (11) is used. This makes the estimation task partly easier, partly harder, compared to an on-line filter. Assuming time invariance gives more accurate estimates since no data forgetting has to be included in the filter. On the other hand, prior information of the very slowly time-varying slip offset from previous drives is not incorporated into the filter. This sometimes leads to biased estimates (slip slope and slip offset overestimated, see (14)) when the excitation is poor.

Each data set contain data from about two minutes, which is close to the time constant of the Kalman filter. That is, the parameter uncertainty using the filter of this section and the Kalman filter should be of the same order.

Test brakes were performed, where the mean deceleration was used as an estimate of μ_{max}. This turned out to work well on slippery roads, but the result for high values on μ_{max} are uncertain.

4.2 Test results for different tires

Figure 6 shows γ and k for several tests, one plot for each tire. We will comment on each plot and explain unexpected results. These can be explained by either poor excitation or the ambiguity in visual inspection of surfaces.

Comments on MXT:

- The asphalt drive with a small $k = 45$ was performed on a salted road after a snow fall and should perhaps be classified as snow or wet asphalt. A test brake showed a small $\mu_{max} = 0.41$.

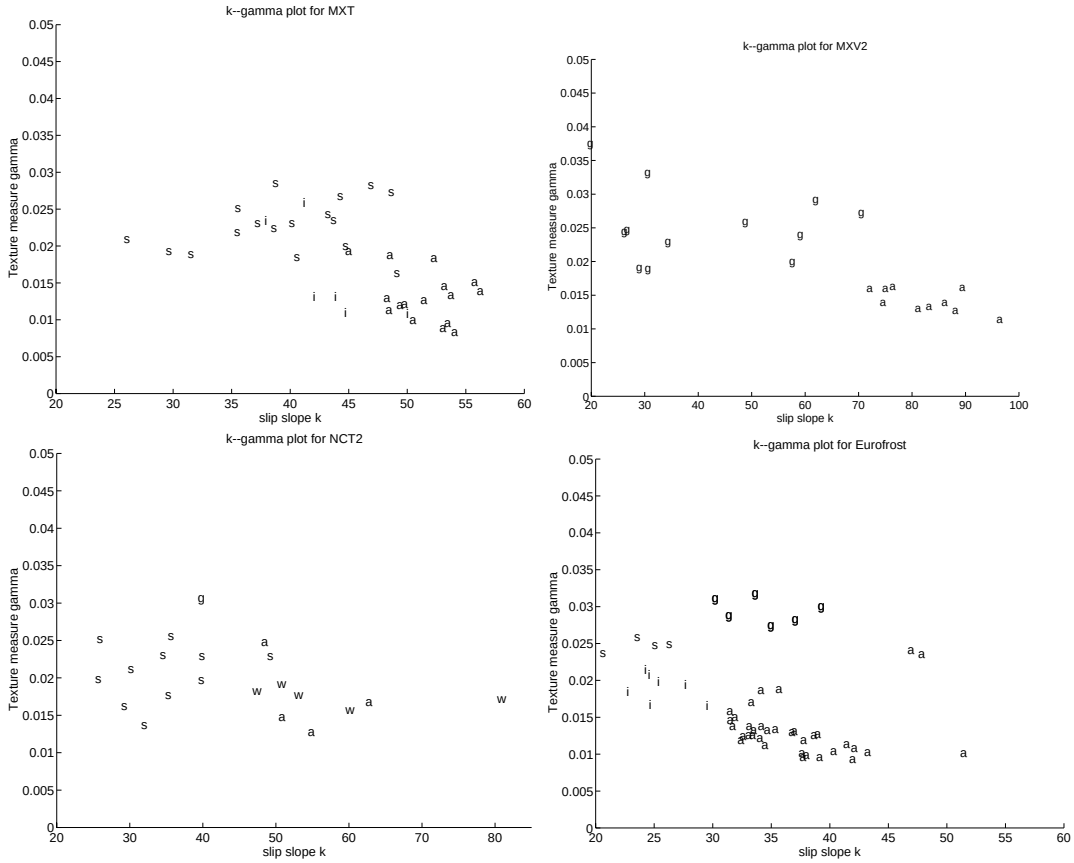

Fig. 6. Slip slope and texture measure as a function of surface

- The snow drives with $k > 40$ were all performed on the same road with friction $\mu_{max} \approx 0.4$. The snow drives with $k < 40$ corresponds to lower friction roads $\mu_{max} = 0.3$ to $\mu_{max} = 0.35$.
- The ice drives are all from the same occasion. High humidity caused traffic problems on a major highway with an invisible ice covered asphalt surface. The friction was $\mu_{max} \approx 0.4$. The prototype successfully gave alarm and a correct friction estimate in this real and dangerous situation.
- Thus, three different friction conditions seem to be distinguished. The friction classes $\mu_{max} < 0.35$, $0.35 < \mu_{max} < 0.45$ and $\mu_{max} > 0.45$ can in almost all cases be distinguished by the classifier $k < 40$, $40 < k < 47$ and $k > 47$.
- All tests have $\gamma < 0.03$.

Comments on MXV2:

- The slip slope is systematically larger here due to the worn tires.
- The slip slope on gravel is smaller than on asphalt and shows a huge variation.
- Gravel drives can be distinguished from asphalt by checking if $\gamma > 0.017$.

Comments on NCT2:

– A k threshold of 45 classifies asphalt and snow correctly.
– The slip slope and offset are over-estimated in one snow drive.
– One wet asphalt drive shows a remarkably high slip slope ($k = 80$). The excitation is very good ($\overline{\mathrm{Var}}(\mu) = 0.050^2$) and model error small ($\sigma = 0.5$) so it is a reliable result.

Comments on Eurofrost:

– This is the most promising result in this report, where all surfaces are well clustered.
– There is a clear difference between asphalt and snow/ice with threshold $k = 30$.
– The distinction between ice and snow is ambiguous. The friction on snow was 0.3 and on the icy surface 0.35. Test brakes shows a certain correlation between μ_{max} and slip slope.
– Gravel roads are characterized by $\gamma > 0.027$.
– The ice drive with the largest slip slope, $k = 29$, is likely to have a significant bias according to Equation (18), since $\mathrm{Var}(\mu) = 0.025^2$.

Clearly, the threshold needed in a classifier differ for different tires. Furthermore, a winter tire with knobs showed a very small slip slope in the order of 15. Therefore, the thresholds must be adaptive with respect to tire changes and wearness. Note, however, that these results support the functionality of a *relative* friction estimator. That is, a skid detector should work with high significance level.

4.3 Influence of external factors

A lot of tests were conducted to examine the influence of external factors. The results of these are summarized below:

– The accuracy of k when a test is repeated at another occasion is in the order of 10%. Since the time constants of both the Kalman filter and the filter used in this section are of the same order, the accuracy of k from the Kalman filter can be expected to 10% as well.
– Cruising with constant speed normally gives a bias less than 10% in k.
– A decrease in tire inflation pressure for a driven (front) wheel of 0.5 bar gives a 20% decrease in k, while a change in a non-driven wheel does not influence the slip slope.
– A change of tire inflation pressure larger than 0.2 bar in any tire, shows up as a change in the offset δ with one per mille. Therefore, abnormal inflation pressure can be detected if the estimated slip offsets on the left and right side differs more than 1 per mille (which is larger than its estimation uncertainty).

- Cold tires and also a cold engine contribute to overestimate k, the actual amount being slightly correlated to outdoor temperature. After 10 km drive the estimate of k has converged to its stationary value.
- The computation of engine torque is accurate only when the torque is almost constant (the model is static) in which case the filter is active. The time constant of the engine is of the order of one second, so a few samples have to be thrown away when the torque is changed.
- The computation of normal force is inaccurate in bends using the simple mechanical model in appendix A.4. This is especially true on the outer wheel, which implies a lower bound on curve radius where the model is valid.
- A change in load, like going from no to three passengers, does not seem to affect the slip slope.

That is, the friction classifier should be inactive the first 10 km of drive, when an abnormal inflation pressure is detected, in bends (detected by a small curve radius) and during non-static torque. The *ad-hoc* rules that have been implemented lead to a 90% availability. The resolution of the slip slope cannot be higher than 10%. A relative friction estimator can, however, be used all the time.

4.4 The classifier and self calibration

The suggested classifier uses the slip slope k and the texture measure γ and has the following form, where we also suggest a *self-calibration* procedure:

(i) If $\gamma > 0.03$, then the surface is gravel ($\mu \approx 0.6$) no matter what k is.
(ii) If $\gamma < 0.03$ and $k > 0.9k_0$, then the surface has high friction ($\mu > 0.7$).
(iii) If $\gamma < 0.03$ and $0.7k_0 < k < 0.9k_0$, then the surface is slippery ($\mu \approx 0.4$).
(iv) If $\gamma < 0.03$ and $k < 0.7k_0$, then the surface is very slippery ($\mu < 0.3$).
(v) In addition to the rules above, use a 10% hysteresis around the limits to avoid repeatedly switching between two states.
(vi) The classifier is inactive the first 10 km and when the tire inflation pressure is detected to be abnormal.
(vii) Detection of abrupt friction changes is done all the time without the need for self calibration.

In a protype developed in this project, the driver information unit consists of a LED display where the number of active LED's is inversely proportional to the μ-value indicated above. Furthermore, the unit alarms for sudden skid when the change detector gives an alarm.

The limit of 0.03 for gravel detection seems to work for reasonably worn tires. Here k_0 is a tire dependent limit which must be adaptive. We suggest to update it to

the current estimate of k each time $\gamma \approx 0.01$ and the excitation is good. These circumstances are characteristic for asphalt roads with little bias on k. This means that the classifier will adapt itself after a tire change once the car enters an asphalt road with acceptable excitation. This is the principle of the self-calibration.

5 Conclusions

An algorithm for estimating tire-road friction during normal driving and using only standard sensors has been presented. The approach works on two-wheel driven vehicles during normal driving. The algorithm is based on a Kalman filter supported by a change detection algorithm to give reliable and accurate estimates of the so called slip slope and, at the same time, to be able to follow abrupt changes quickly.

Results from extensive tests were presented. There is no doubt that two, probably three, different friction conditions can be classified from an estimated slip slope. Especially changes in friction can be detected quite accurately. To get a more accurate relationship between slip slope and friction, an additional friction sensor is needed to replace the test brakes used here. The algorithm was designed to work during normal driving and availability is restricted in that the algorithm is inactive during sharp bends, braking, torque changes, skidding and when the engine is cold.

This work may be seen as a thorough verification of the slip-based approach and there remain a number of topics for further research before a possible implementation. Firstly, the availability can be increased. A dynamical engine model would allow data immediately after a torque change to be used. With a better model for the normal forces, sharper bends can be tolerated. An accelerometer and gyro, or an image based sensor of velocity, are needed if information during skidding and braking is to be included. Finally, measurements of engine and outdoor temperature might be used to improve availability before the engine is warm-up. Secondly, the benefits of increasing the estimation accuracy using additional hardware should be studied. A gyro would increase the accuracy of curve radius during bends, which affects one of the filter inputs. Then, also the slip angle can be used during bends in a similar way as the longitudinal slip. Very accurate friction estimation is probably only possible during high excitation as braking and spinning, so available friction information from the ABS and a traction control system during high excitation should be incorporated in an implementation.

The major problem with this approach if absolute and not only relative friction information is needed, is the sensitivity to tire type and condition. Before implementation, the matter of self-calibration should be carefully investigated and the suggestion presented herein evaluated on a long-term basis.

A Modelling

The inputs to the filter are the slip s and the friction coefficient F_f/N. We will here describe how the three quantities s, F_f, N can be computed. Related formulas for ground vehicles can be found in [20,8].

A.1 Slip bias

A first problem in computing the slip (1) is that the wheel radii are not the same, so we cannot compute the wheel velocities directly. The reason why the wheel radii differ is a combination of different load on each wheel, different tire inflation pressure, perhaps even differently worn tires and other factors. Suppose we define the relative difference in wheel radius on both ends of the car by δ_w

$$r_f = r_r(1 - \delta_w). \tag{A.1}$$

Here the indeces f and r stand for front and rear, respectively. The slip is then

$$s = \frac{v_f - v_r}{v_r} = \frac{v_f}{v_r} - 1 = \frac{\omega_f r_f}{\omega_r r_r} - 1 = \frac{\omega_f}{\omega_r}(1 - \delta_w) - 1. \tag{A.2}$$

Since δ_w is unknown, we must confine with using the quantity s_m defined by

$$s_m = \frac{\omega_f}{\omega_r} - 1 \tag{A.3}$$

as input to the filter. Combining (A.3) and (A.2) gives

$$s_m = \frac{s + \delta_w}{1 - \delta_w} = (s + \delta_w)(1 + \delta_w + \delta_w^2 + ...) \approx s + \delta_w. \tag{A.4}$$

Since both s and δ_w are of the order of a few per mille and the presence of other uncertainties in the model make that we can dismiss with higher order terms. This means that the slip offset δ defined in (4) and the relative difference in δ_w defined in (A.1) can be considered to be the same. That is, we have derived the source of the observed offset in slip measurement. The difference in wheel radii thus leads to a (slowly time-varying) offset in the slip measurements.

While driving in a curve, all four wheels have different angular velocities. This is easily seen from Figure A.1, where the different wheel radii to the momentary pole are defined.

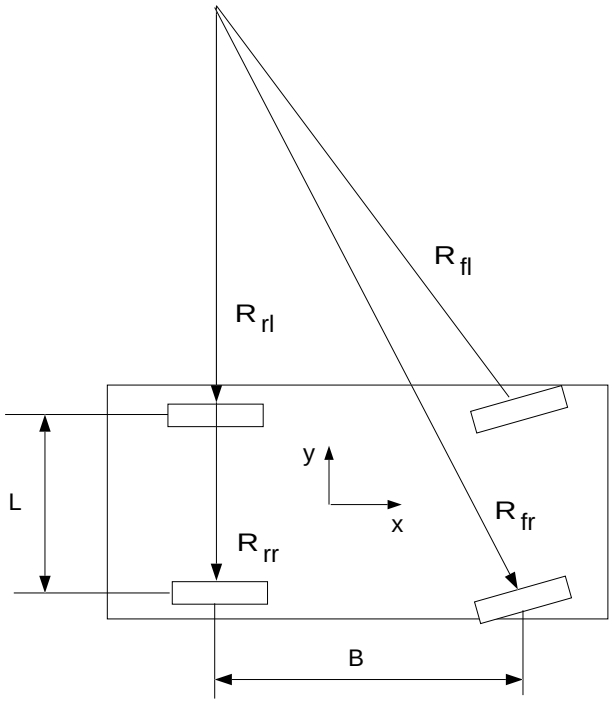

Fig. A.1. Geometric relations for the wheel velocities during cornering.

By introducing the radius $R = R_{rr}$, simple geometry gives

$$\begin{aligned} R_{rr} &= R \\ R_{rl} &= R - L \\ R_{fr} &= \sqrt{R^2 + B^2} \\ R_{fr} &= \sqrt{(R-L)^2 + B^2}. \end{aligned}$$

We can use geometry and the difference of the non-driven rear wheels to compute the curve radius R. Define the angular velocity around the curve center as ω_z. Using the relations

$$\begin{aligned} \omega_{rl} r_{rl} &= \omega_z R_{rl} = \omega_z (R - L) \\ \omega_{rr} r_{rr} &= \omega_z R_{rr} = \omega_z R \end{aligned} \tag{A.5}$$

and assuming equal wheel radii, $r_{rl} = r_{rr} = r_{fl} = r_{fr} = r_w$, give

$$R = \frac{L}{1 - \frac{\omega_{rl}}{\omega_{rr}}}. \tag{A.6}$$

Here it should be remarked that the curvature R^{-1} rather than R itself shall be computed to allow straight ahead driving ($R^{-1} = 0$). The value of R is not very accurate, since the denominator is as sensitive to differences in wheel radii as the slip. A gyro would give a much more accurate value. A complication which is difficult to model is the asymmetric compression of the inner/outer wheels in curves.

The same relations can be used for computing the z-component of the angular velocity of the car, ω_z. Solving (A.5) for ω_z gives

$$\omega_z = \frac{(\omega_{rl} - \omega_{rr})r_w}{L} \tag{A.7}$$

We will now compute the slip values on the right and left side. Here we will distinguish the different front and rear wheel radii in order to get accurate expressions on this very important parameter. We immediately get the velocity of the driven wheels as

$$\begin{aligned} v_{fr} &= \omega_z \sqrt{R^2 + B^2} \\ v_{fl} &= \omega_z \sqrt{(R - L)^2 + B^2}. \end{aligned} \tag{A.8}$$

This can be written as

$$\begin{aligned} v_{fr} &= \omega_{rr} r_{rr} \sqrt{1 + \frac{B^2}{L^2}(\frac{\omega_{rl}}{\omega_{rr}} - 1)^2} \\ v_{fl} &= \omega_{rl} r_{rl} \sqrt{1 + \frac{B^2}{L^2}(1 - \frac{\omega_{rr}}{\omega_{rl}})^2}. \end{aligned} \tag{A.9}$$

Notice that the geometry just introduces a correction factor in the velocity computations. The slip at each driven wheel is thus

$$\begin{aligned} s_{fr} &= \frac{\omega_{fr} r_{fr}}{v_{fr}} - 1 = \frac{\omega_{fr} r_{fr}}{\omega_{rr} r_{rr} \sqrt{1 + \frac{B^2}{L^2}(\frac{\omega_{rl}}{\omega_{rr}} - 1)^2}} - 1 \\ s_{fl} &= \frac{\omega_{fl} r_{fl}}{v_{fl}} - 1 = \frac{\omega_{fl} r_{fl}}{\omega_{rl} r_{rl} \sqrt{1 + \frac{B^2}{L^2}(1 - \frac{\omega_{rr}}{\omega_{rl}})^2}} - 1 \end{aligned} \tag{A.10}$$

Because we only know the approximate value r_w on the wheel radii, we use the definition (4) and the ideas developed in subsection A.1. We then get

$$
\begin{aligned}
s_{frm} &= \frac{\omega_{fr}}{\omega_{rr}\sqrt{1+\frac{B^2}{L^2}(\frac{\omega_{rl}}{\omega_{rr}}-1)^2}} - 1 \\
s_{flm} &= \frac{\omega_{fl}}{\omega_{rl}\sqrt{1+\frac{B^2}{L^2}(1-\frac{\omega_{rr}}{\omega_{rl}})^2}} - 1
\end{aligned}
\tag{A.11}
$$

where

$$s_{frm} \approx s_{fr} + \delta_r \tag{A.12}$$

$$s_{flm} \approx s_{fl} + \delta_l \tag{A.13}$$

Again, we obtain the standard slip expression with a correction factor depending on the geometry.

We have here assumed that the car is front wheel driven. However, similar expressions for how to compensate for cornering are easily derived for rear wheel driven cars as well.

A.3 Determining the traction force

The engine's torque T is computed from measured injection time and engine speed using a tabulated model. Since the model was obtained in a test bench using static engine load, we do not expect good accuracy when the measured quantities vary quickly. Neglecting the inertia of the wheels and driving line, the traction force is given by $F_f = 0.5\,T\,i/r$, where r is the wheel radius and i the gearing ratio determined by comparing engine speed and wheel speed.

A.4 Normal forces during accelerations

Basically, the normal forces are given by the mass of the car and the position of the center of gravity. Nevertheless, the normal forces are changed drastically during for instance cornering. We will derive some relations, but we want to point out that some of these only give marginal effects and there might be other ones which are more important. However, most of the problems experienced in cornering vanished when using the formulas presented below, although there is a tendency to overcompensate. That is, the formulas give normal forces that are too large on the outer wheels.

If the velocity is constant, the normal force is given by the car's mass and geometry. A reasonable assumption is that the time constants of the accelerations are considerably larger than for the dynamics of the springs. We can then express the normal forces as static relations. With notation as in Figure A.2, the total normal force at the two driven front wheels is

$$N_f = Mg\frac{x_b}{x_b + x_f}.$$

If we take the effects of acceleration F_x and air drag F_a into account, we get

$$N_f = \frac{Mgx_b + F_x z_g - F_a(z_g - z_a)}{x_b + x_f}. \tag{A.14}$$

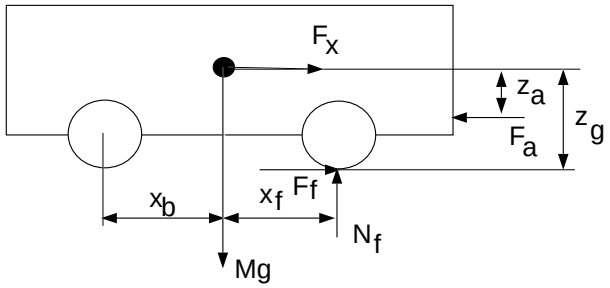

Fig. A.2. Geometric relations of the normal force and the acceleration.

In curves we have the lateral acceleration $F_y = \frac{mv^2}{R}$, with notation as in Figure A.1. This acceleration gives the contribution $F_y\frac{z_g}{y_f}$ to the normal force on the outer wheels of which the front wheel gets the contribution $F_y\frac{z_g}{y_f}\frac{x_b}{x_b+x_f}$, and we get

$$N_{fl} = \frac{Mgx_b + F_x z_g - F_a(z_g - z_a) - 2F_y\frac{z_g}{y_f}x_b}{2(x_b + x_f)} \tag{A.15}$$

$$N_{fr} = \frac{Mgx_b + F_x z_g - F_a(z_g - z_a) + 2F_y\frac{z_g}{y_f}x_b}{2(x_b + x_f)}, \tag{A.16}$$

where we can use

$$\begin{aligned} F_a &= \rho c_w A_x v^2 \\ F_x &= Ma_x \\ F_y &= \frac{m\omega_{rr}^2 r_w^2}{R}. \end{aligned} \tag{A.17}$$

The air drag F_a depends on the front area A_x, the air density ρ and the aerodynamical coefficient c_w. Here R is given by (A.6). We have so far assumed a turn to the left, but notice that these expression still holds for right turns (where R is negative).

References

[1] S.E. Shladover. Research and development needs for advanced vehicle control systems. *IEEE Micro*, pages 11–19, February 1993.

[2] U. Eichhorn and J. Roth. Prediction and monitoring of tyre/road friction. In *Proceedings of FISITA*, London, June 1992.

[3] A. Svärdström. Classification of road surface using a neural net (in swedish). Technical Report UPTEC 93 056R, Uppsala University, Uppsala, Sweden, June 1993.

[4] U. Kiencke. Realtime estimation of adhesion characteristic between tyres and road. In *Proceedings of the IFAC Congress*, pages 15–18, Sydney, 1993.

[5] T. Dieckmann. Assessment of road grip by way of measured wheel variables. In *Proceedings of FISITA*, London, June 1992.

[6] F. Gustafsson. Slip-based estimation of tire - road friction. In *Proc. on the 1995 European Control Conference, Rome*, pages 725–730, 1995.

[7] Vehicle dynamics terminology. SAE J670e, Society of Automotive Engineers, 1978.

[8] J.Y. Wong. *Theory of Ground Vehicles.* John Wiley & Sons, New York, 2 edition, 1993.

[9] U. Kiencke and A. Daiss. Estimation of tyre friction for enhanced ABS-systems. In *Proceedings of the AVEG Congress*, Tokyo, 1994.

[10] E. Bakker, L. Nyborg, and H.B. Pacejka. Tyre modelling for use in vehicle dynamic studies. Society of Automotive Engineers, paper 870421, 1987.

[11] S. van Huffel and J. Vandewalle. *The total least squares problem.* SIAM, Philadelphia, 1991.

[12] L. Ljung and T Söderström. *Theory and Practice of Recursive Identification.* MIT Press, Cambridge MA, 1983.

[13] B.D.O. Anderson and J.B. Moore. *Optimal Filtering.* Prentice Hall, Englewood Cliffs, NJ., 1979.

[14] E.S Page. Continuous inspection schemes. *Biometrika*, 41:100–115, 1954.

[15] M. Basseville and I.V. Nikiforov. *Detection of abrupt changes: theory and application.* Information and system science series. Prentice Hall, Englewood Cliffs, NJ., 1993.

[16] A.S. Willsky and H.L. Jones. A generalized likelihood ratio approach to the detection and estimation of jumps in linear systems. *IEEE Transactions on Automatic Control*, pages 108–112, 1976.

[17] F. Gustafsson. The marginalized likelihood ratio test for detecting abrupt changes. *IEEE Tr. on Automatic Control*, 41(1):66–78, 1996.

[18] F. Gustafsson. Estimation and change detection of tire—road friction using the wheel slip. In *Proc. of CCA, 1996*, 1996.

[19] F. Gustafsson. Identification of sparse linear regressions. In *Proc. of IFAC, San Fracisco, 1996*, 1996.

[20] Automotive handbook. 3 edition, Robert Bosch GmbH, 1993.